Polarisation-mode coupling in (100)-cut Nd:YAG

Aaron M^{c}Kay[1⋆], Judith M. Dawes[1] and Jong-Dae Park[2]

[1] *Centre for Lasers and Applications, Department of Physics Macquarie University, Sydney, NSW 2109, Australia*

[2] *Department of Physics, Pai-Chai University, Daejon, Korea. 302-735*

⋆ *Corresponding author: aaron@ics.mq.edu.au*

Abstract: We investigate the polarisation-mode dynamics and Lamb's mode coupling constant for orthogonally polarised laser states in a dual-mode (100)-cut Nd:YAG laser with feedback, and compare with an anisotropic rate equation model. The anisotropic (100)-cut Nd:YAG exhibits thermally-induced depolarisation and polarisation-mode coupling dependent on the pump polarisation, crystal angle and laser polarisation directions. Here, the links between the depolarisation and polarisation-mode coupling are discussed with reference to a rate equation model which includes gain anisotropy in a quasi-isotropic laser cavity.

OCIS codes: (140.3580) Lasers, solid-state; (140.3530) Lasers, neodymium.

References and links

1. C. L. Tang, H. Statz, and G. deMars, "Spectral output and spiking behavor of solid-state lasers," J. Appl. Phys. **34**, 2289–2295 (1963).
2. K. Otsuka, P. Mandel, S. Bielawski, D. Derozier, and P. Glorieux, "Alternate time scale in multimode lasers," Phys. Rev. A**46**, 1692–1696 (1992).
3. M. Brunel, A. Amon, and M. Vallet, "Dual-polarization microchip laser at 1.53 μm," Opt. Lett. **30**, 2418–2420 (2005).
4. L. Morvan, N. D. Lai, D. Dolfi, J.-P. Huignard, M. Brunel, F. Bretenaker, and A. Le Floch, "Building blocks for a two-frequency laser lidar-radar: a preliminary study," Appl. Opt. **41**, 5702–5712 (2002).
5. W. Du, S. Zhang, and Y. Li, "Principles and realization of a novel instrument for high performance displacement measurement—nanometer laser ruler," Opt. Laser Eng. **43**, 1214-1225 (2005).
6. M. Brunel, O. Emile, F. Bretenaker, A. Le Floch, B. Ferrand, and E. Molva, "Tunable two-frequency lasers for lifetime measurements," Opt. Rev. **4**, 550-552 (1997).
7. M. Alouini, F. Bretenaker, M. Brunel, A. Le Floch, M. Vallet, and P. Thony, "Existence of two coupling constants in microchip lasers," Opt. Lett. **25**, 896–898 (2000).
8. W. E. Lamb, "Theory of an optical maser," Phys. Rev. A**134**, A1429–A1450 (1964).
9. R. Bayerer, J. Heber, and D. Mateika, "Crystal-field analysis of Tb^{3+} doped Yttrium aluminium garnet using site-selective polarized spectroscopy," Z. Phys. B Con. Mat. **64**, 201–210 (1986).
10. R. Dalgliesh, A. D. May, and G. Stephan, "Polarization states of a single-mode (microchip) Nd^{3+}:YAG laser—Part II: Comparison of Theory and Experiment," IEEE J. Quantum Electron. **34**, 1493–1502 (1998).
11. R. Dalgliesh, A. D. May, and G. Stephan, "Polarization states of a single-mode (microchip) Nd^{3+}:YAG laser—Part I: Theory," IEEE J. Quantum Electron. **34**, 1485–1492 (1998).
12. A. M^{c}Kay, P. Dekker, D. W. Coutts, and J. M. Dawes, "Enhanced self-heterodyne performance using a Nd-doped ceramic YAG laser," Opt. Commun. **272**, 425–430 (2007).
13. G. W. Baxter, J. M. Dawes, P. Dekker, and D. S. Knowles, "Dual-polarization frequency-modulated laser source," IEEE Photon Technol. Lett. **8**, 1015–1017 (1996).
14. M. Brunel, M. Vallet, A. Le Floch, and F. Bretenaker, "Differential measurement of the coupling constant between laser eigenstates," Appl. Phys. Lett. **70**, 2070-2072 (1997).

15. M. A. van Eijkelenborg, C. A. Scharama, and J. P. Woerdman, "Quantum mechanical diffusion of the polarization of a laser," Opt. Commun. **119**, 97–103 (1995).
16. W. Koechner *Solid-state laser engineering* (Springer, 1999).
17. G. Verschaffelt, G. van der Sande, J. Danckaert, T. Erneux, B. Ségard, and P. Glorieux, "Polarization switching in Nd:YAG lasers by means of modulating the pump polarization," Proc. SPIE **6184**, 61841V-1–61841V-9 (2006).
18. I. Shoji and T. Taira, "Intrinsic reduction of the depolarization loss in solid-state lasers by use of a (110)-cut $Y_3Al_5O_{12}$ crystal," Appl. Phys. Lett. **80**, 3048–3050 (2002).
19. I. B. Mukhin, O. V. Palashov, E. A. Khazanov, and I. A. Ivanov, "Influence of the orientation of a crystal on thermal polarization effects in high-power solid-state lasers," JETP Lett. **V81**, 90–94 (2005).

1. Introduction

Multimode laser dynamics has been an intriguing subject from the early days of experimental observation. Tang *et al.* [1] studied two-mode lasers considering the cross-saturation effects due to spatial hole burning, and predicted self-organised collective behaviour in transient oscillations of two-mode lasers where the total output behaves, in essence, like a single-mode laser. Otsuka *et al.* [2] extended their study to include cross-saturation in the multimode rate equations, yielding additional dynamical oscillation frequencies associated with anti-phase motions. Recently dual-mode lasers have been applied to microwave photonics [3, 4], high precision metrology [5] and spectroscopy [6]. Alouini *et al.* [7] observed two types of coupling in microchip lasers—between longitudinal modes and between orthogonally-linearly-polarised eigenstates. They interpreted their results using Lamb's mode-coupling constant, which was derived to analyse the coupling between longitudinal modes in gas lasers [8]. In this model the atom-light interaction was assumed to be isotropic, so that gain anisotropy was neglected.

However, in solid-state lasers this assumption is no longer valid; in crystalline lasers, the active atoms are oriented according to the crystal symmetry. A yttrium aluminum garnet (YAG) crystal, in particular, has a cubic unit cell that contains 8 formula units with the dopant (here Nd^{3+}-ions) substituting for the yttrium on the dodecahedral D_2 sites [9]. Relative to the cubic unit cell (or sub-unit cell [10]), the neodymium ions are oriented along the face diagonals in 6 possible directions. The (100)-cut Nd:YAG therefore, with the optical axis along the *z*-axis, has a set of orthogonally-oriented dipoles at $\pm 45^\circ$ with respect to the *x*–*y* axes of the cubic unit cell and 2 more sets oriented at 0° and 90°. Dalgliesh *et al.* [11] developed a microscopic theory of the polarisation states of a single-mode laser showing the phase relationship between the components of the dipole transition moments, considering the populations at six non-equivalent sites. They also estimated the relative strength of the dipole moment components at the lasing and pump wavelengths.

In our work, the coupling between polarisation modes arises from the mode competition for the same excited ions in Nd:YAG, and is heavily dependent on saturation and spatial hole burning effects within the laser medium. We extend the work of Alouini *et al.* [7] and Dalgliesh *et al.* [10, 11] to establish an anisotropic rate equation model that incorporates the orientations of the Nd^{3+}-ions to study the behaviour of dual-mode Nd:YAG lasers. These lasers naturally oscillate on two orthogonal polarisations, with dual optical frequencies determined by the (tunable) birefringence in the cavity, with frequency separations of up to half the axial mode spacing. The lasers can generate a beat frequency in the RF or microwave wavelength region [3, 12], and may be modulated to give frequency-modulated output [13].

If one considers polarisation-mode coupling as the result of the interaction between orthogonally oriented gain ions, the (100)-cut Nd:YAG crystal is ideal for investigating mode coupling effects, since its dipoles are oriented along the *x*–*y* axes of the cubic unit cell and at $\pm 45^\circ$. In this paper we use the crystal angle to investigate the effect of polarisation-mode coupling and related anti-phase dynamics in dual-polarised lasers. We show that the gain anisotropy (that governs polarisation-mode coupling) is related to the polarisation rotation from thermally-

induced birefringence (or depolarisation). Isotropic gain is shown to increase the pump-induced depolarisation and correspondingly the anisotropic gain minimises the depolarisation.

2. Anisotropic rate equation model

The anisotropic characteristics of solid-state lasers can be modelled using the Maxwell-Bloch equations from the coherent density matrix equations [11] but quickly become complicated when considering multiple modes. Fortunately these equations can be reduced to relatively straightforward rate equations using some appropriate assumptions. The atomic polarisations are obtained as a function of the population difference between the upper and lower energy levels. For dual orthogonally-polarised lasers, further simplifications can be made if one assumes that the mode-beating frequency is large compared to the inverse of the population inversion lifetime, and the side bands generated by mode beating are not resonant with the laser cavity.

Accounting for the laser-atom interaction anisotropy in a (100)-cut Nd:YAG crystal, the rate equations for the photon density ϕ_j for the j-polarised beam for $j = x$ or y, and the population inversion n^i for each of the i atomic sites are:

$$\frac{\mathrm{d}\phi_j}{\mathrm{d}t} = \frac{\phi_j}{t_r}\left(2\sum_{i=1}^{6}\left(c^i_{jq}\sigma_q + c^i_{jr}\sigma_r + c^i_{js}\sigma_s\right)n^i l - \ln(1/R) - L_j\right) \quad (1)$$

$$\frac{\mathrm{d}n^i}{\mathrm{d}t} = \Lambda^i - \gamma c\Big(\left(c^i_{xq}\sigma_q + c^i_{xr}\sigma_r + c^i_{xs}\sigma_s\right)\phi_x + \left(c^i_{yq}\sigma_q + c^i_{yr}\sigma_r + c^i_{ys}\sigma_s\right)\phi_y\Big)n^i - \frac{n^i}{\tau_s} \quad (2)$$

where the cavity round trip time t_r is 0.88 ns, the output coupler reflectivity R is 0.97, and the cavity losses for x- and y-polarised beams L_j are 0.03 to 0.1. γ is the population inversion parameter, and $\tau_s = 230\ \mu$s is the lifetime of population inversion. The effective stimulated emission cross-section can be calculated if the stimulated emission cross-sections σ_q, σ_r, σ_s along the atomic axes ($\hat{q}$, $\hat{r}$, $\hat{s}$) are known, by using a coordinate transformation (for example c^i_{xq}, c^i_{xr},...) from the atomic axis frame to the laboratory frame [9]. Λ^i is the pumping rate to the i-th group of ions, which depends on the atomic orientation, absorption cross-section along atomic axes, and the pump laser polarisation. The pumping rate is given by:

$$\Lambda^i = \frac{2\gamma_{\mathrm{abs}}}{\gamma^2_{\mathrm{abs}} + \Delta\omega^2}\Big[p^2_{pq}(E^2_{pxq} + E^2_{pyq}) + p^2_{pr}(E^2_{pxr} + E^2_{pyr}) + p^2_{ps}(E^2_{pxs} + E^2_{pys}) + 2(p^2_{pq}E_{pxq}E_{pyq} + p^2_{pr}E_{pxr}E_{pyr} + p^2_{ps}E_{pxs}E_{pys})\Big] \quad (3)$$

where the absorption half bandwidth γ_{abs} is 2×10^9 s^{-1}, the pump laser frequency detuning $\Delta\omega$ is 0 Hz from the absorption peak. E_{pxq}, E_{pxr}, E_{pxs} are the electric field components of the x-directed electric field E_x along the atomic axes for the pump laser and similarly for the y-directed electric field component. The dipole moments at the pump wavelength along the atomic axes are denoted p_{pq}, p_{pr}, p_{ps} and were adopted from Ref. [10], as were values for σ_q, σ_r, σ_s. To simulate modulated feedback we used an additional loss term $L_x(1 + \varepsilon\cos(2\pi f_{mod}t))$ in place of the cavity loss term (L_x) in Eq. (1), where the feedback amplitude ε is $\sim 10^{-5}$ and the modulation frequency f_{mod} is 1 kHz.

3. Experimental laser arrangement and mode-coupling experiments

To investigate the polarisation-mode coupling dynamics and the validity of our anisotropic rate equation model, a laser with a 5-cm long linear cavity was set up incorporating a dielectric input mirror with high transmission at 808 nm and high reflectivity (HR) at 1064 nm; a 5-mm long 1-at.% doped (100)-cut Nd:YAG crystal in a rotatable mount; a 21-mm long z-cut $LiNbO_3$

electro-optic crystal (LN); a 0.5-mm thick 30% reflecting étalon to maintain a single axial mode; and a 97% HR output mirror with radius of curvature of 15 cm. The pump source was a multi-mode fiber-coupled laser diode, whose polarisation was scrambled with a depolarising prism and then re-polarised by a Glan-Laser polarising cube and rotated using a half wave-plate (HWP). The polarisation axes of the dual-mode laser were fixed by applying a transverse electric field (~ 500 kV/m) across the LN. To measure the mode coupling [12] we used a polarised feedback path consisting of a HWP and polarising beam splitter to select a polarisation, optical density filters to adjust the feedback, and a piezo-driven mirror. The path length of the feedback arm was modulated at 1 kHz to modulate the gain of one laser eigen-polarisation.

In dual-mode lasers a second relaxation oscillation appears in the low frequency noise spectrum [2, 3]. In general, this second or "anti-phase" relaxation oscillation is the result of the interaction between multiple oscillating modes. In dual polarisation lasers these oscillations are found in both orthogonal modes, oscillating out of phase with each other. They are typically much weaker (~ 30 dB) than the "in-phase" relaxation oscillations which are dominated by the equivalent single-mode laser characteristics. When mixed on a photodiode, the anti-phase components of the polarised relaxation oscillations cancel, and they are typically not detectable when monitored individually. There have been several techniques used to investigate these anti-phase dynamics [e.g., 3]. We investigate the anti-phase dynamics by introducing a slight perturbation caused by applying ~ 10 ppm polarisation-sensitive feedback. This perturbation caused additional frequency-modulated noise destroying the negative correlation between the anti-phase motions of the two polarisation eigenstates. This allowed the two relaxation oscillation frequencies to be viewed simultaneously on a single unpolarised photodetector and radio-frequency spectrum analyser. Weaker feedback caused a weak out-of-phase modulation to the laser modes, produced primarily by the cross-saturation and mode coupling effects [12, 14]. Stronger feedback caused polarisation switching [15, 17].

4. Results

We compared the experimental results of the anti- (triangles) and in-phase (squares) relaxation oscillations with the linearised solutions of Eqs. (1–3) (solid lines) in Fig. 1(a) using the parameters in Sec. 2. The experimental data (10 ppm feedback) show good agreement with our theory. We also applied the relationship between the relaxation oscillations and Lamb's coupling constant from Brunel *et al.* [Eq. (2) in 3] to our experimental and theoretical data of Fig. 1(a) to determine the polarisation-mode coupling as a function of incident pump power as shown in Fig. 1(b). There is close agreement to the measured results within experimental error. Eqs. (1–3) were also solved numerically with the modulated loss term. Comparing the modelled intensity of both polarisations, we calculated a coupling constant which was consistent with our experimental results.

By varying the relative (100)-cut YAG angle to the laser polarisation axes the amount of coupling between orthogonal polarisation modes can be controlled. Thus, in Fig. 2(a) we modelled the effect of the polarisation-mode coupling as a function of the crystal angle for a set of fixed polarisation axes. Experimentally, the laser polarisation axes were fixed by applying 500 V across the LN crystal and aligning the pump polarisation to $45^\circ \pm 2^\circ$ with respect to the induced laser axes. The gain crystal was rotated about the optical axis to measure the polarisation-mode coupling, shown as red squares in Fig. 2(a). After each rotation increment the laser mirrors and étalon were realigned to give equal power in each of the two orthogonal modes. As the crystal axes approached either 0° or 90° the étalon was adjusted to counteract the extra gain along the *x* or *y* axes of the cubic unit cell by introducing additional losses to one mode. When the axes of the cubic unit cell were aligned to the laser polarisation directions, the laser action was restricted to a single polarisation, so the coupling constant was not measurable.

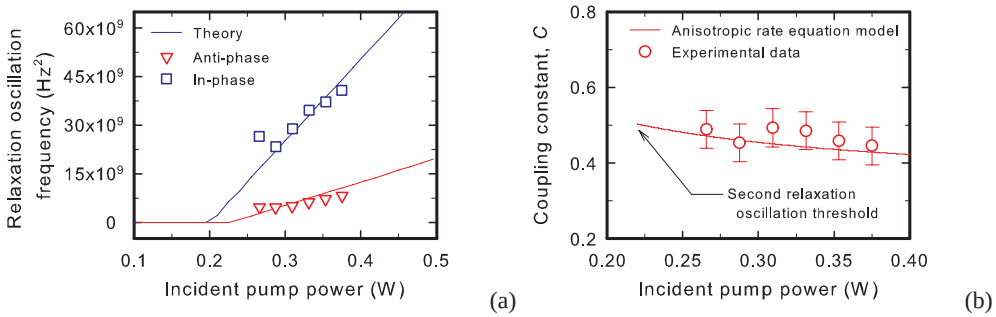

Fig. 1. **(a)** In- and anti-phase relaxation oscillations due to the polarisation-mode coupling dynamics as a function of the incident pump power. **(b)** Experimental and modelled coupling constant as a function of incident pump power. Crystal and pump polarisation angles were set to 56° and 45° relative to the laser axes respectively.

Laser gain materials without strong dominating gain axes, such as the various doped glasses [16], tend to suffer from thermally-induced depolarisation and have larger coupling constants [3], than materials with a strong dominating gain axis [16]. It has been shown in (100)-cut Nd:YAG that depolarisation can be minimised by rotating the gain crystal to particular angles [18]. Depolarisation has typically been defined as the ratio of the power transferred into an "undesired" polarisation to that of the initial or desired polarisation [16, 19] whereas polarisation-mode coupling is generally regarded as the ratio of the polarised power of each mode coupled destructively (i.e. via anti-phase motions) into the alternate orthogonal mode. In Fig. 2(a) we also plot the depolarisation, in the form of the pump-induced birefringence. The depolarisation model and parameters used, apart from pumping level and the crystal dimensions, were adopted from Shoji *et al.* [18]. Experimentally, using a similar technique as illustrated in Ref. [19] and probing with a tightly focused ($\omega_p \approx 30\ \mu$m) pump, the experimental polarisation rotation or relative pump-induced birefringence was determined. The measurement was limited by the contrast ratio of the analysing polariser and the relatively low pump powers used (compared to Refs. [18, 19]), however there is a visible trend between the modelled and experimental pump-induced birefringence. Clearly the polarisation-mode coupling and the induced birefringence of the (100)-cut Nd:YAG crystal follow similar sinusoidal trends although out-of-phase. In Refs. [16, 18, 19], the underlying cause of depolarisation is thermal stresses arising from the pump absorption in the gain medium. This absorption, especially in end-pumped lasers, generates a strong spatially-dependent thermal gradient in the crystal. As a result of the photoelastic effect, a birefringent profile is produced in the gain medium proportional to both the direction and the magnitude of the temperature gradient. Even in low power systems, such as ours, the birefringence caused by the depolarisation can be relatively large. We estimate the birefringence to be of order 10^{-6} which is equivalent to ~ 100 V applied to the LN crystal. Also the photoelastic effect provokes mechanical stresses on the dodecahedral neodymium sites and their neighbouring oxygen atoms, essentially causing distortions to the gain ion sites and lifting the degeneracy of the energy states. Because polarisation-mode coupling depends on birefringence (as a ratio of the two overlapping polarisations) then it also shows a contribution from the photoelastic effect. Thus pump-induced depolarisation and gain-dominated polarisation mode-coupling phenomena are related in (100)-cut Nd:YAG crystals.

The link between the depolarisation and the coupling is further emphasised in Fig. 2(b) where we show the effect of the pump polarisation direction on the two orthogonal modes and the an-

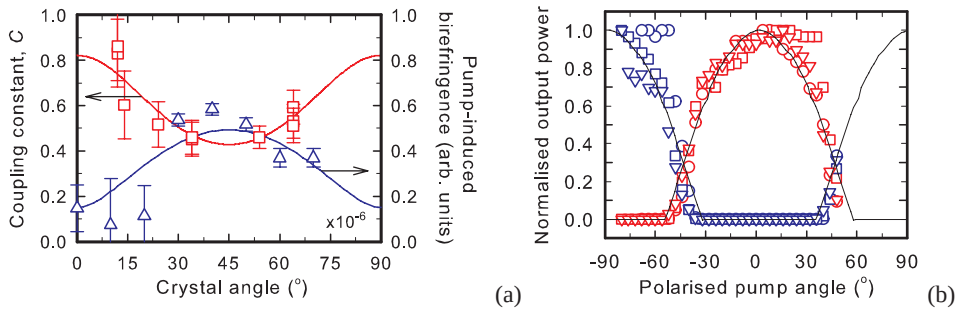

Fig. 2. **(a)** Comparison of polarisation-mode coupling (modelled—red line and experimental data—squares) and pump-induced birefringence (modelled—blue line and experimental data—triangles) as a function of crystal angle in a (100)-cut Nd:YAG laser. Pump polarisation direction at 45° to the laser polarisation axes. **(b)** Influence of the pump polarisation on the normalised orthogonal polarisation modes at a crystal angle of 45° with the incident pump power set to 240 mW (circles), 310 mW (squares) and 380 mW (triangles). Red and blue data points refer to the orthogonal polarisation directions.

gles at which the (100)-cut crystal lases readily on either (or both) modes. In this experiment the laser polarisation axes were maintained as before by applying a voltage across the LN crystal, however no effort with the étalon was made to counteract the anisotropic gain or to control the modes simultaneously oscillating. The (100)-cut Nd:YAG crystal was aligned so that the cubic cell axes were 45° to the laser polarisation axes. As outlined in Sec. 3, the pump polarisation was controlled by the angle of the HWP in the collimated region of the pump beam. The output of the (100)-cut Nd:YAG laser was separated into its polarisation components aligned along the laser axes using a polarising beam splitter and monitored on two closely-matched photodiodes and plotted in Fig. 2(b). Fig. 2(b) shows the regions of isotropic gain where both polarisations naturally oscillate. Recalling from Sec. 1 that the dipoles are aligned along the six possible face diagonals of the cubic unit cell, we assign a population inversion to each of the six possible ion directions. For the (100)-cut crystal aligned at 45°, the two orthogonal laser polarisations are exactly collinear with two of the six population inversions. These populations share no component with the opposite polarisation, and therefore have little effect on the polarisation-mode coupling. Both laser polarisations compete for the remaining four directed population inversions, leading to stronger polarisation mode coupling at lower pump powers, as seen in Fig. 1(b). At substantially higher absorbed pump powers the photoelastic effect applies, perturbing the cubic structure of the Nd:YAG crystal so that the orientations of the population inversions change accordingly. The polarisations therefore would not compete so directly for their gain and hence the polarisation-mode coupling decreases with increasing photoelastic effect (and pump-induced birefringence).

5. Conclusions

We have shown excellent experimental agreement with our model. The properties of polarisation-mode coupling and cross-saturation in the (100)-cut Nd:YAG have been explored using the anti-phase dynamics of an anisotropic gain material. Although our models suggest a broad parameter space of coupling variables, experimentally the dominating sets of orthogonally-oriented gain ions in (100)-cut Nd:YAG limited the dual-polarisation regime within the laser to crystal angles with weak mode coupling.